

Figure 1: Drop in mass as a function of time in an as grown $8.5 \mu\text{m}$ thick polypyrrole film. The $\frac{1}{2}$ slope in the log-log plot at the bottom suggests that mass loss is diffusion limited. The blue points in the top figure show the actual measured mass loss, while the red line is the corrected mass loss, accounting for the dropping of two polymer flakes from the weighing pan.

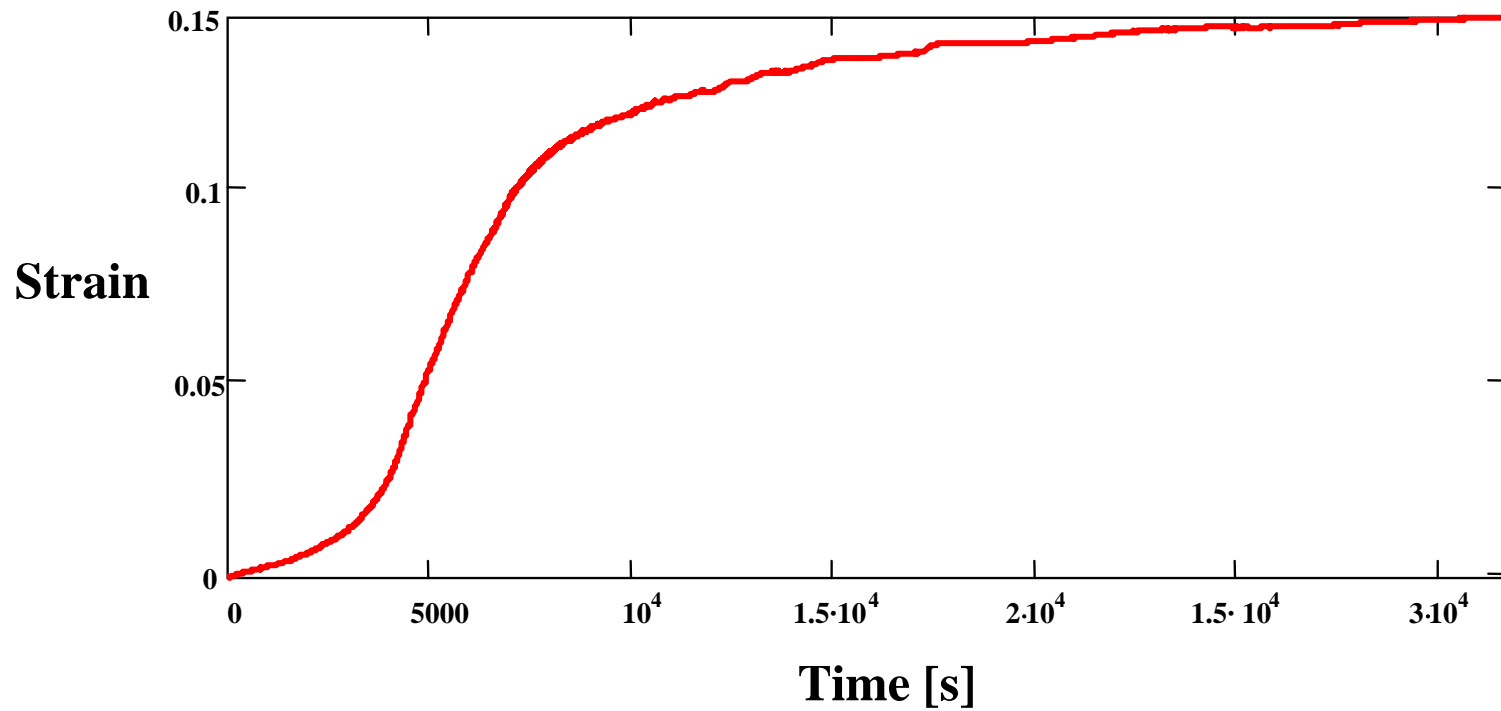


Figure 2: Strain induced in an 8.5 μm thick film held at 3 MPa upon soaking in 0.3 M tetraethylammonium hexafluorophosphate in propylene carbonate. Creep tests performed on previously soaked films produce an extension of less than 2 % over the same time period, indicating that most of the observed strain upon soaking is a result of contact with the electrolyte. During the swelling admittance measurements were made, as shown in Figure 10, about an equilibrium potential of 0.43 V vs. SCE (saturated calomel electrode).

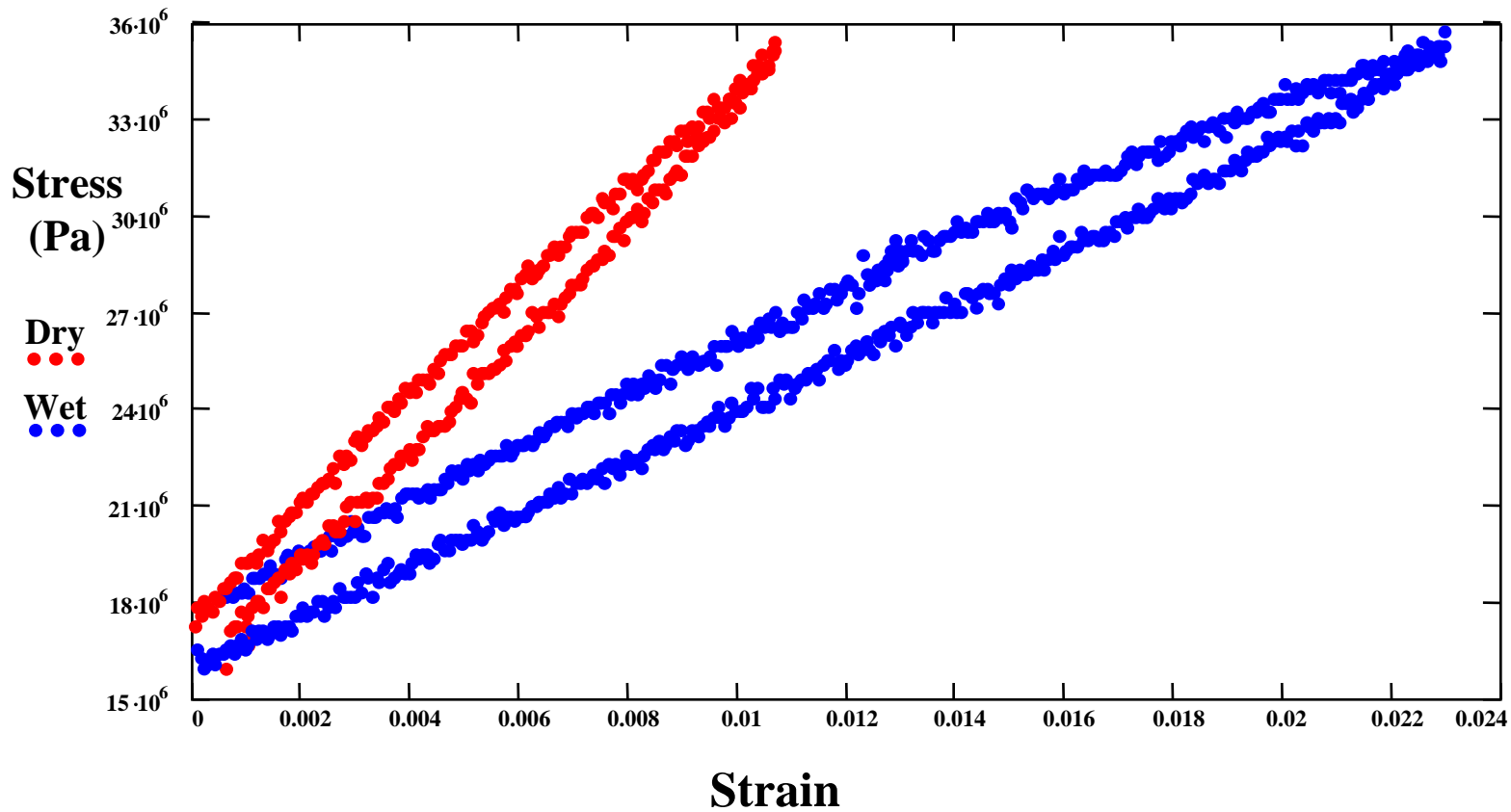


Figure 3: Stress/strain curves in an 8.5 mm thick film before and one day after immersion into 0.3 M tetraethylammonium hexafluorophosphate in propylene carbonate. The strain rate is $4.8 \times 10^{-4} \text{ s}^{-1}$, and the wet stiffness was taken at $V_{eq} = 0.43 \text{ V}$ vs. SCE.

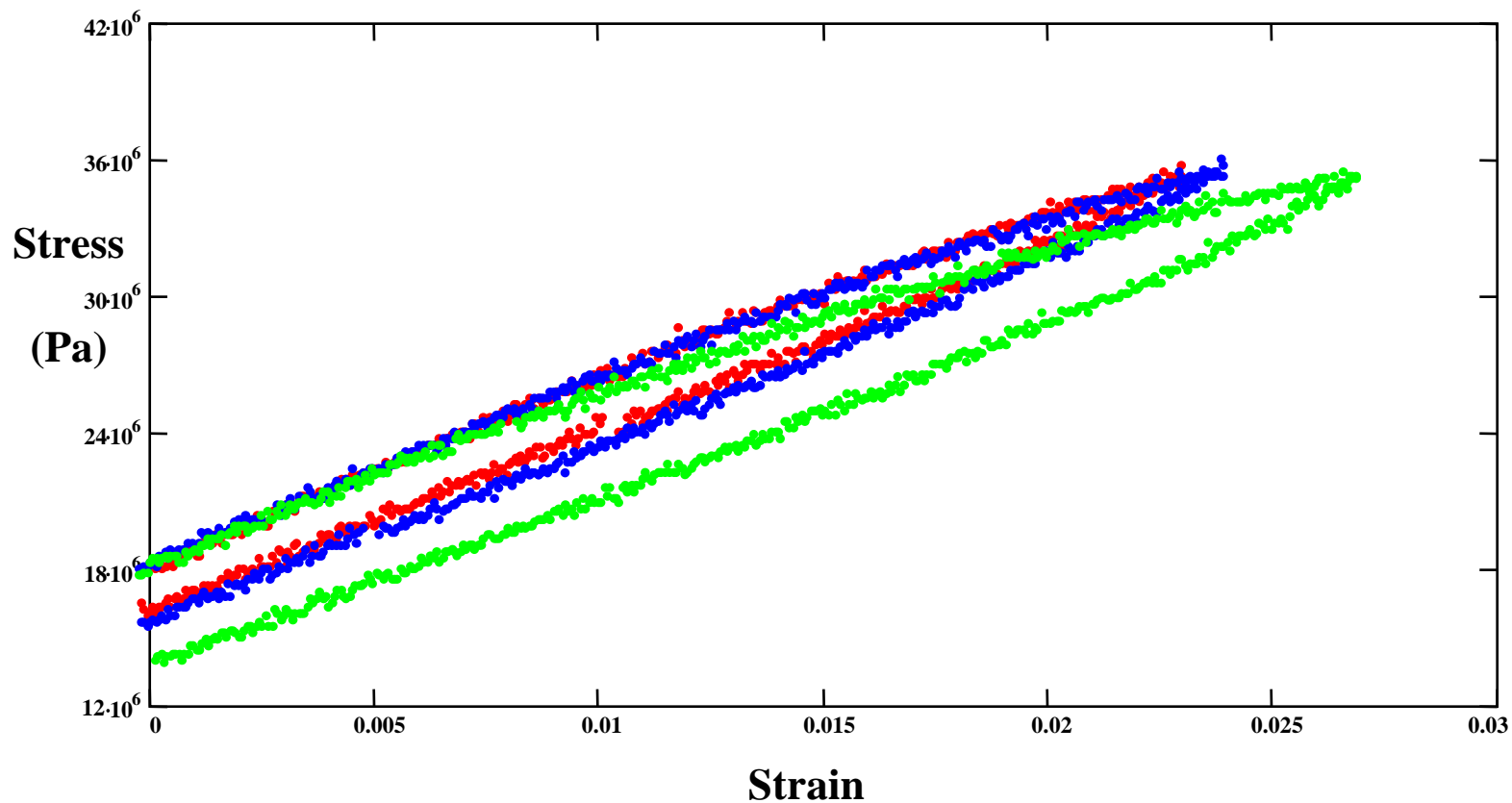


Figure 4: Stress/strain curves in an 8.5 μm thick film in 0.3 M tetraethylammonium hexafluorophosphate in propylene carbonate, indicating the apparent visco-elastic nature of the polypyrrole samples. Strain rates are $4.8 \times 10^{-4} \text{ s}^{-1}$ (red), $2.8 \times 10^{-4} \text{ s}^{-1}$ (blue), and $0.98 \times 10^{-4} \text{ s}^{-1}$ (green). The applied potential, V_{eq} is 0.43 V vs. SCE.

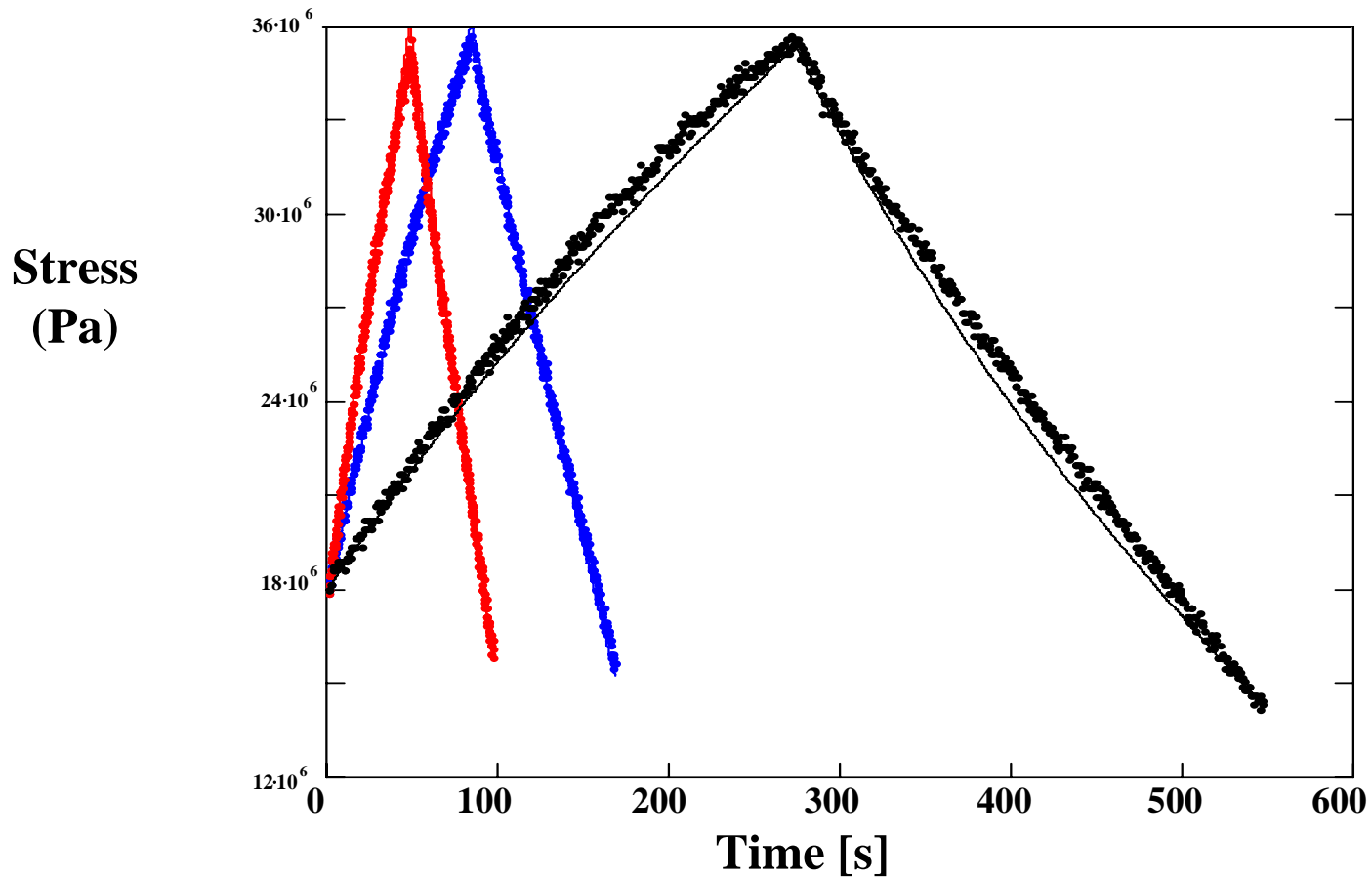


Figure 5: The stress strain data from Figure 4 is replotted in time. Strain rates are $4.8 \times 10^{-4} \text{ s}^{-1}$ (red), $2.8 \times 10^{-4} \text{ s}^{-1}$ (blue), and $0.98 \times 10^{-4} \text{ s}^{-1}$ (black). A visco-elastic model (solid lines) has been fit to the data, suggesting linear response over the range of time scales investigated. The model parameters have values of $E_1=0.83 \text{ MPa}$, $E_2= 1.1 \text{ GPa}$, and $b=300 \text{ GPa}\cdot\text{s}$.

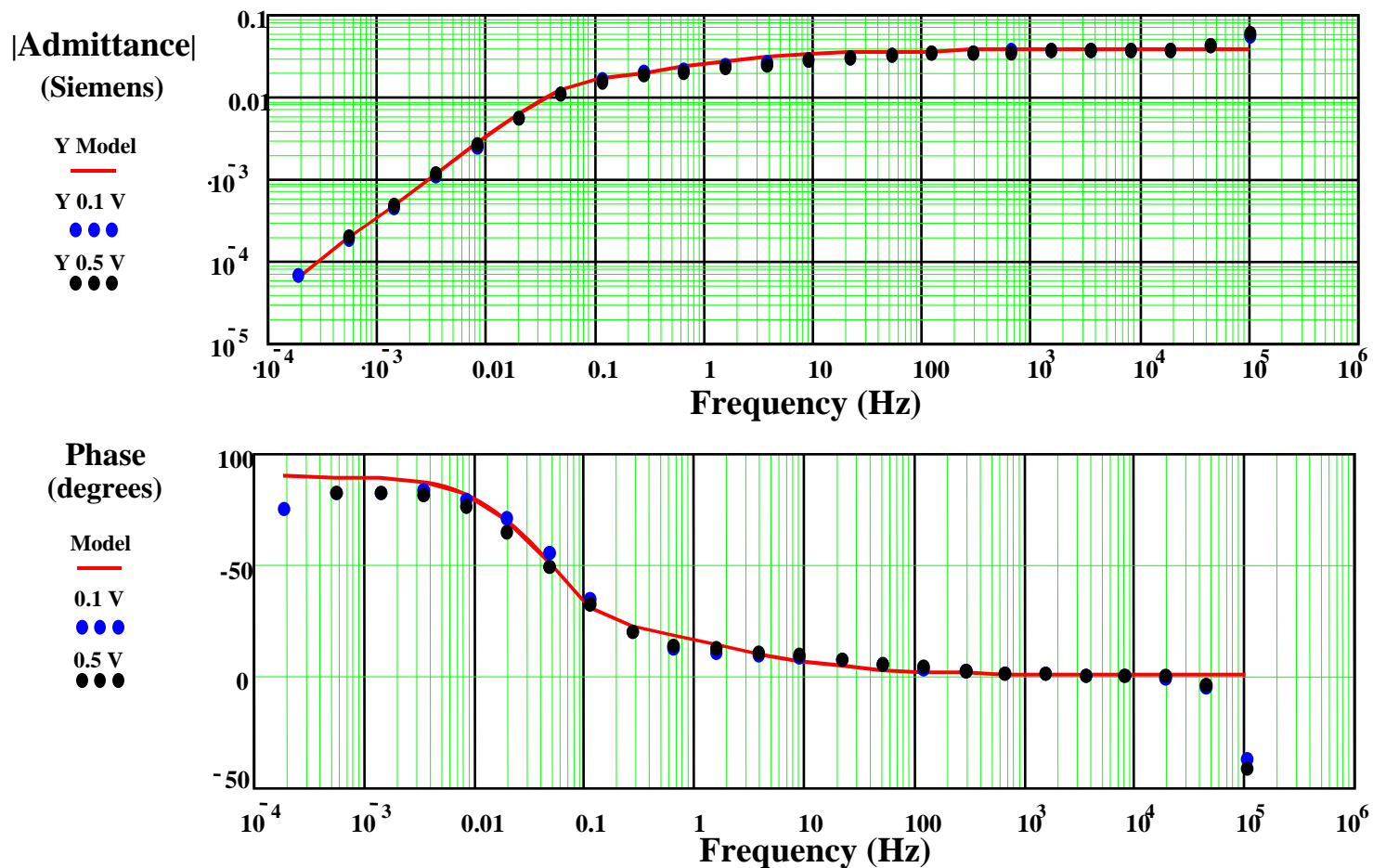


Figure 6: Polypyrrole film admittance measured using swept sine amplitudes of 0.1 V (blue) and 0.5 V (black) peak about . The red line is a model fit. The film employed is $8.5 \mu\text{m}$ thick in 0.37 M tetraethylammonium hexafluorophosphate in propylene carbonate. $V_{eq} = -0.20 \text{ V}$ vs. Ag/AgClO_4 .

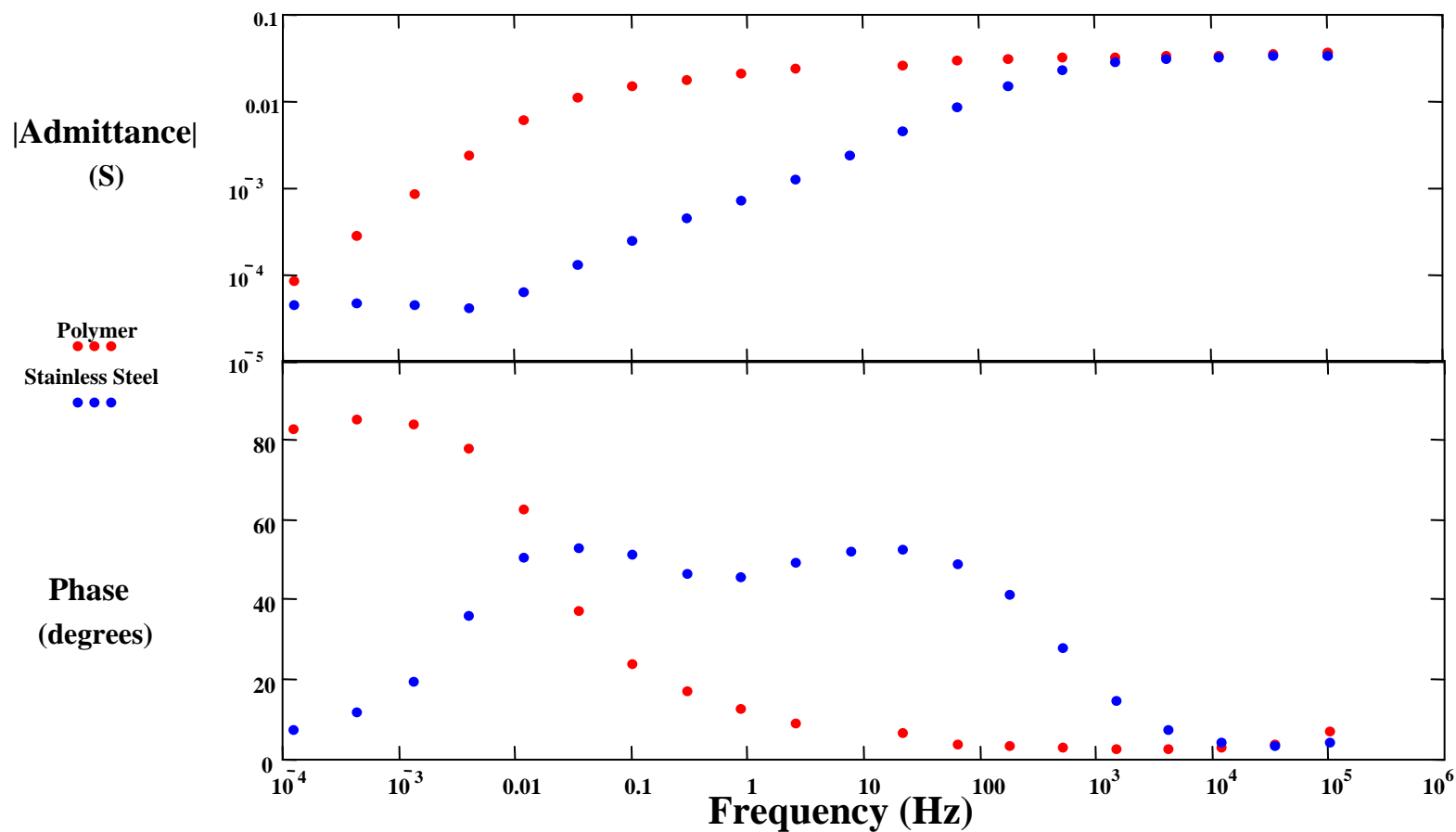


Figure 7: Comparison of admittance obtained from an 8.5 μm thick polymer and a stainless steel electrode of identical surface areas. The fact that the admittance of the stainless electrode is significantly smaller at intermediate and low frequencies suggests that surface reactions and end effects are relatively insignificant. A 0.1 V amplitude is employed about $V_{eq} = 0.43$ V vs. SCE.

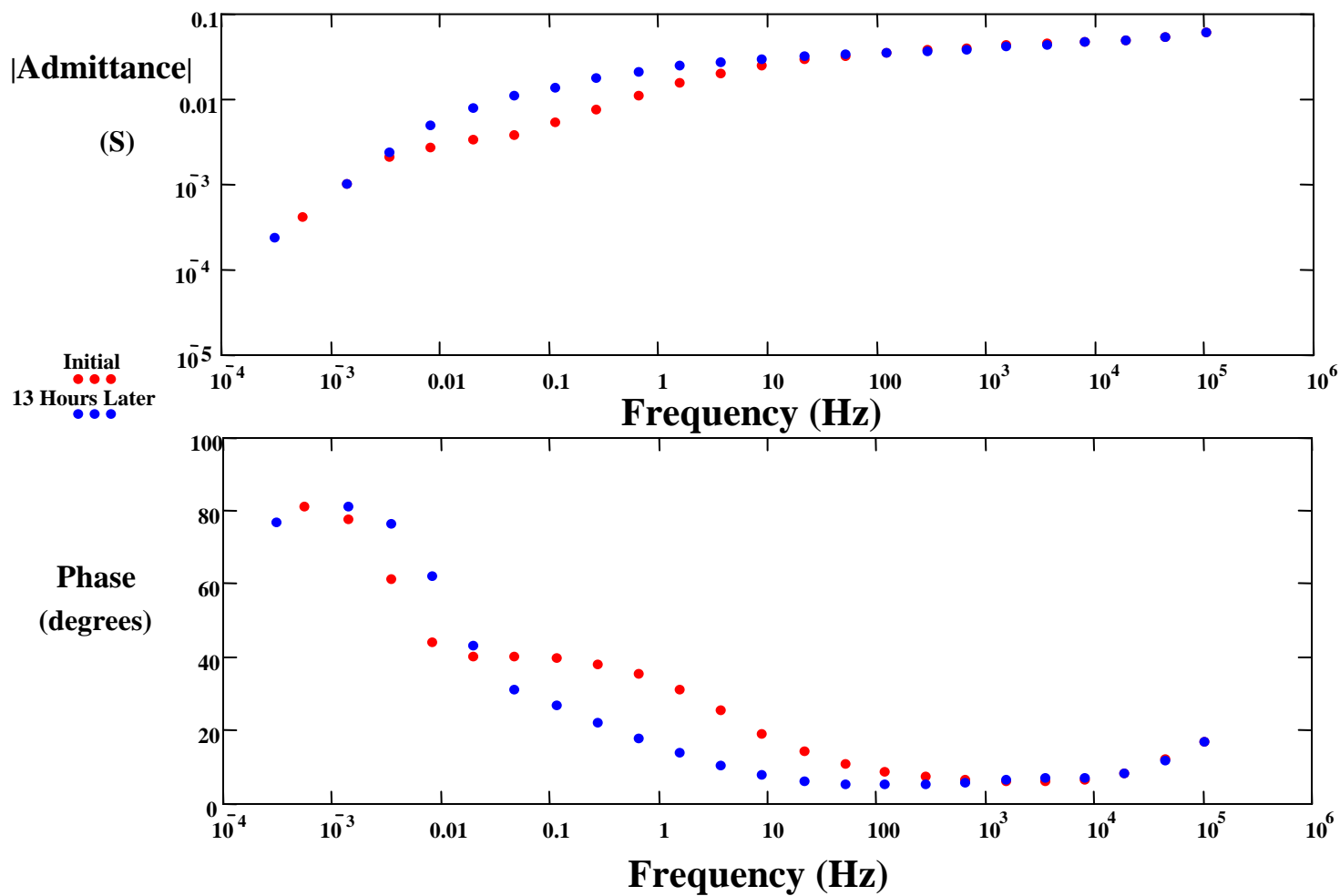


Figure 8: Admittance upon immersion of a 12.5 μm thick film into 0.3 M electrolyte (red) and that taken 13 hours later (blue), indicating a time-dependent response. $V_{eq} = -0.2$ V vs. Ag/AgClO₄.

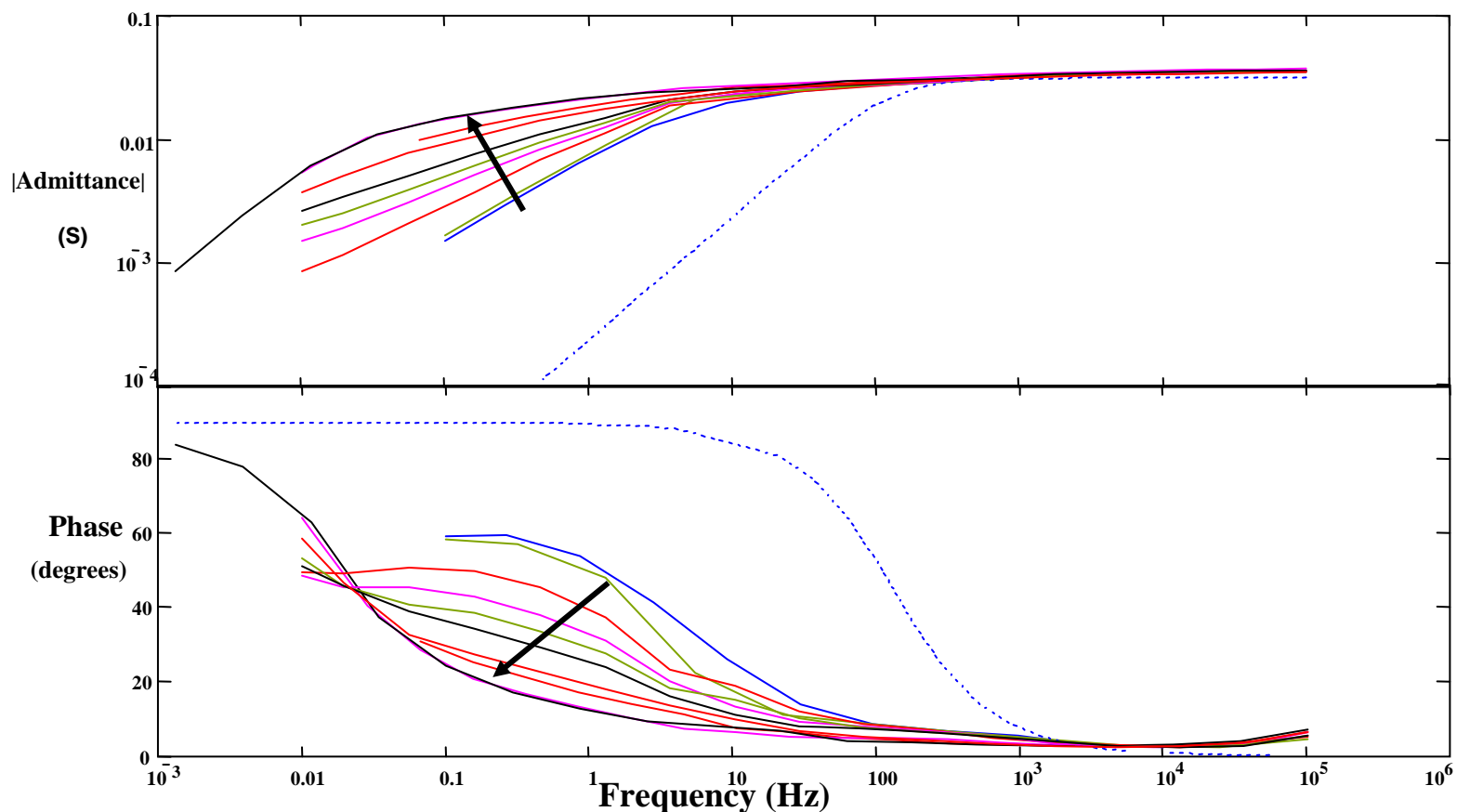


Figure 9: Admittance progression as a function of time after immersion of an 8.5 μm thick film into 0.3 M $(\text{C}_2\text{H}_5)_4\text{NPF}_6$ in propylene carbonate. Solid curves represent data computed at 10, 20, 42, 68, 74, 81, 101, 107, 147, and 680 minutes after immersion, with time increasing in the direction indicated by the arrows. The dashed lines are first order models displayed for comparison. 0.1 V amplitudes are employed about $V_{eq} = 0.43$ V vs. SCE.

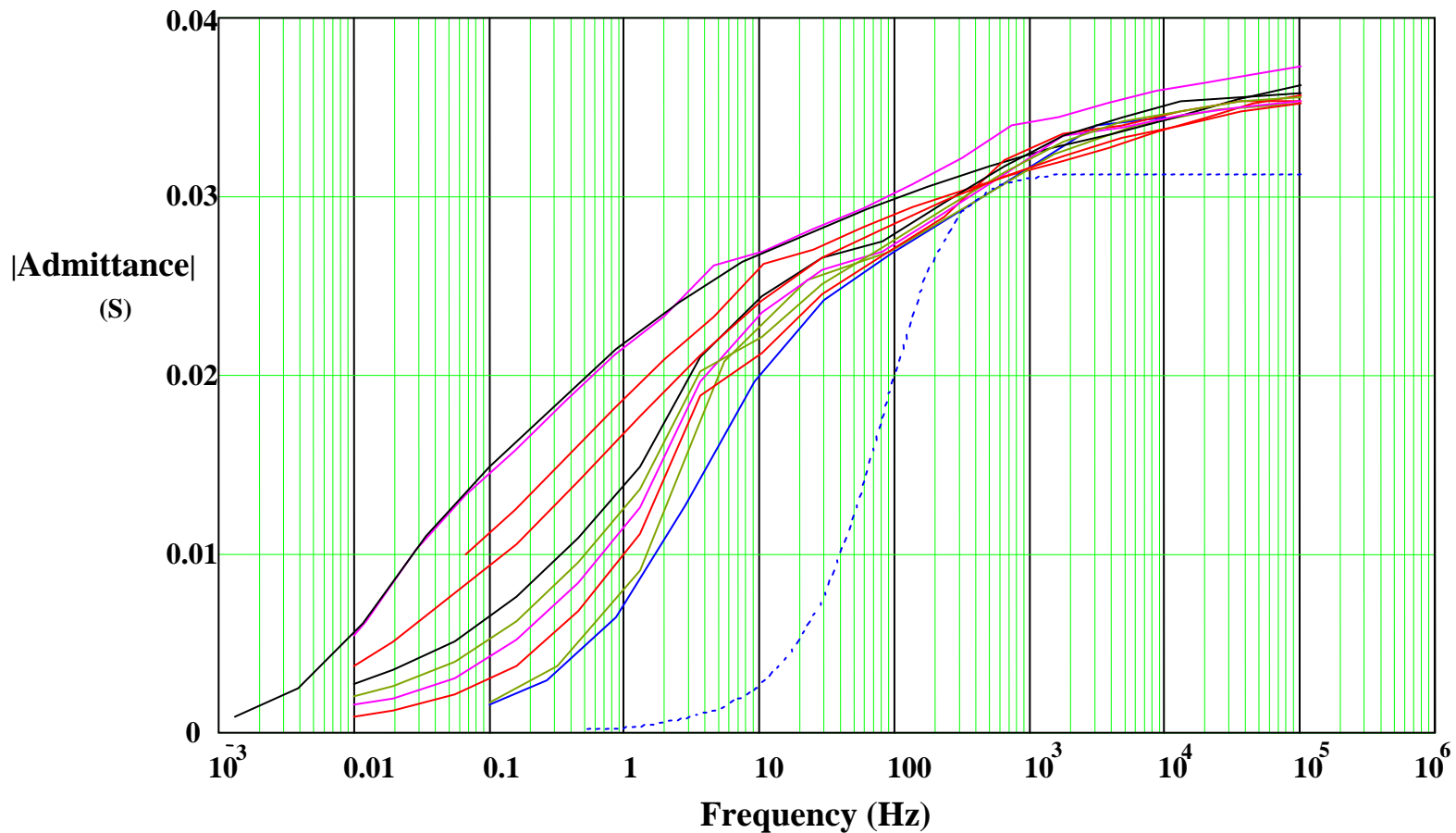


Figure 10: Admittance gain progression as a function of time after immersion of an 8.5 mm thick film into 0.3 M $(C_2H_5)_4NPF_6$ in propylene carbonate, as in Figure 9, but with gain plotted on a linear scale. The first order model (dashed line) is used to obtain an upper bound on double layer capacitance.

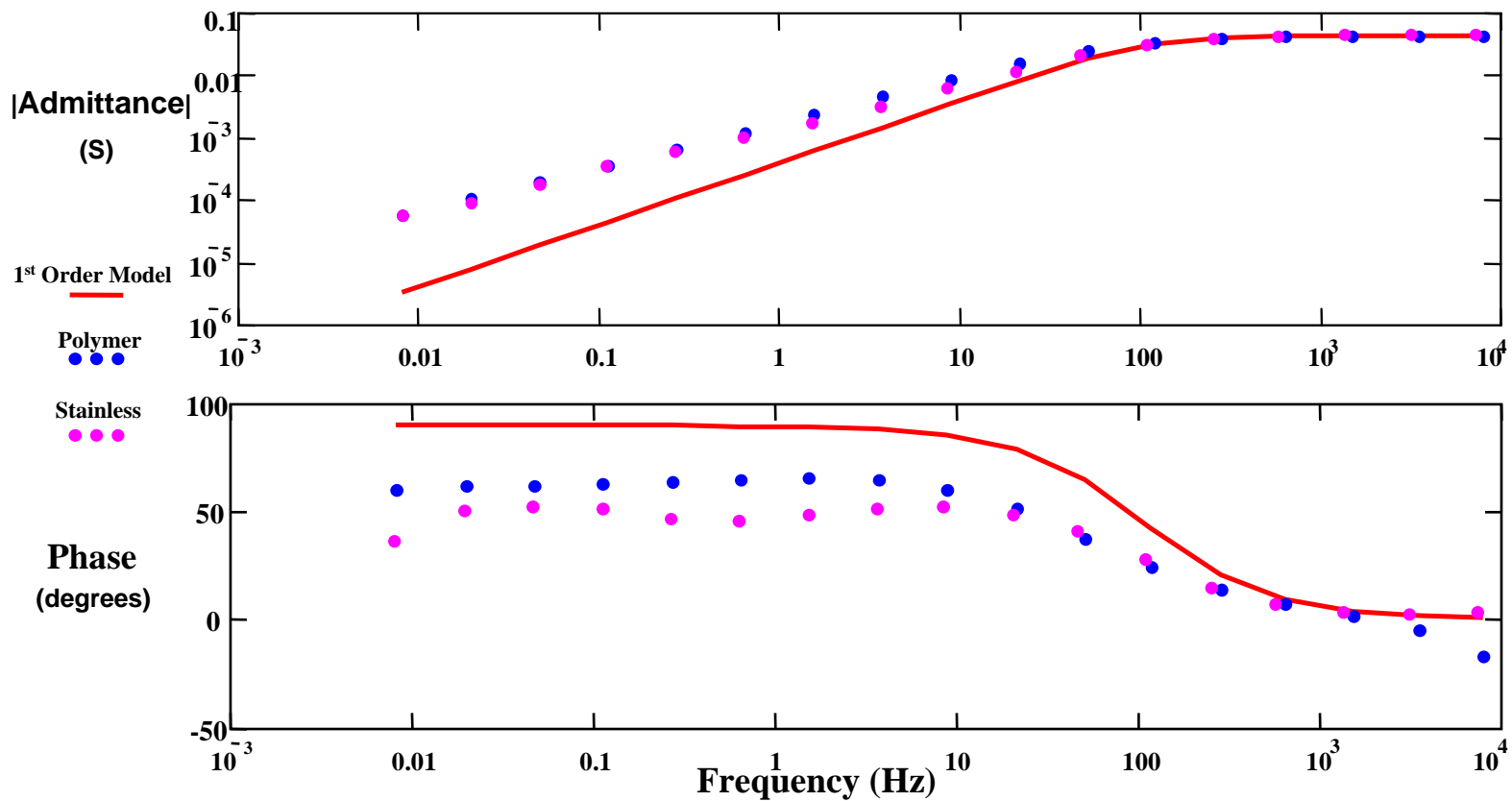


Figure 11: Admittance of a 51 μm thick, 1 year and 4 month old polypyrrole film (blue dots). The first order model (red line) is used to obtain an estimate of double layer capacitance. The results are compared with the response of the stainless steel electrode (Figure 10), which has been shifted in frequency and scaled in magnitude for easier comparison. The similarity between the polymer response and the stainless admittance suggests that the admittance of the aged polypyrrole film is primarily a result of surface effects rather than dopant flux. $V_{eq} = -0.44$ V vs. Ag/AgClO_4 .

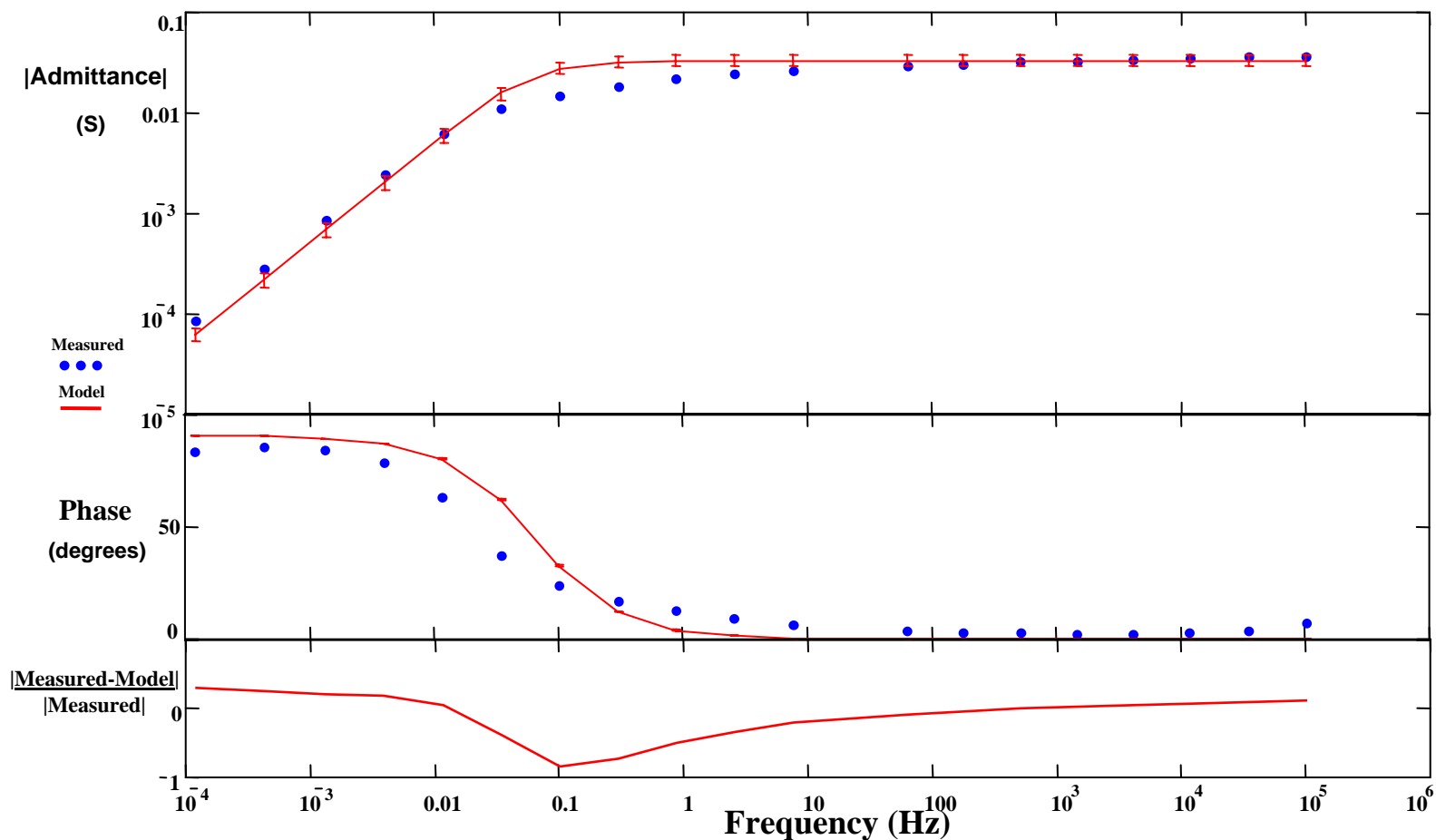


Figure 12: Admittance of an 8.5 μm thick, polypyrrole film and a first order model (red). The bottom plot shows the relative difference between the model prediction and the measured response. The first order model provides a relatively good description of the response at low and high frequencies. $V_{eq} = 0.43$ V vs. SCE.

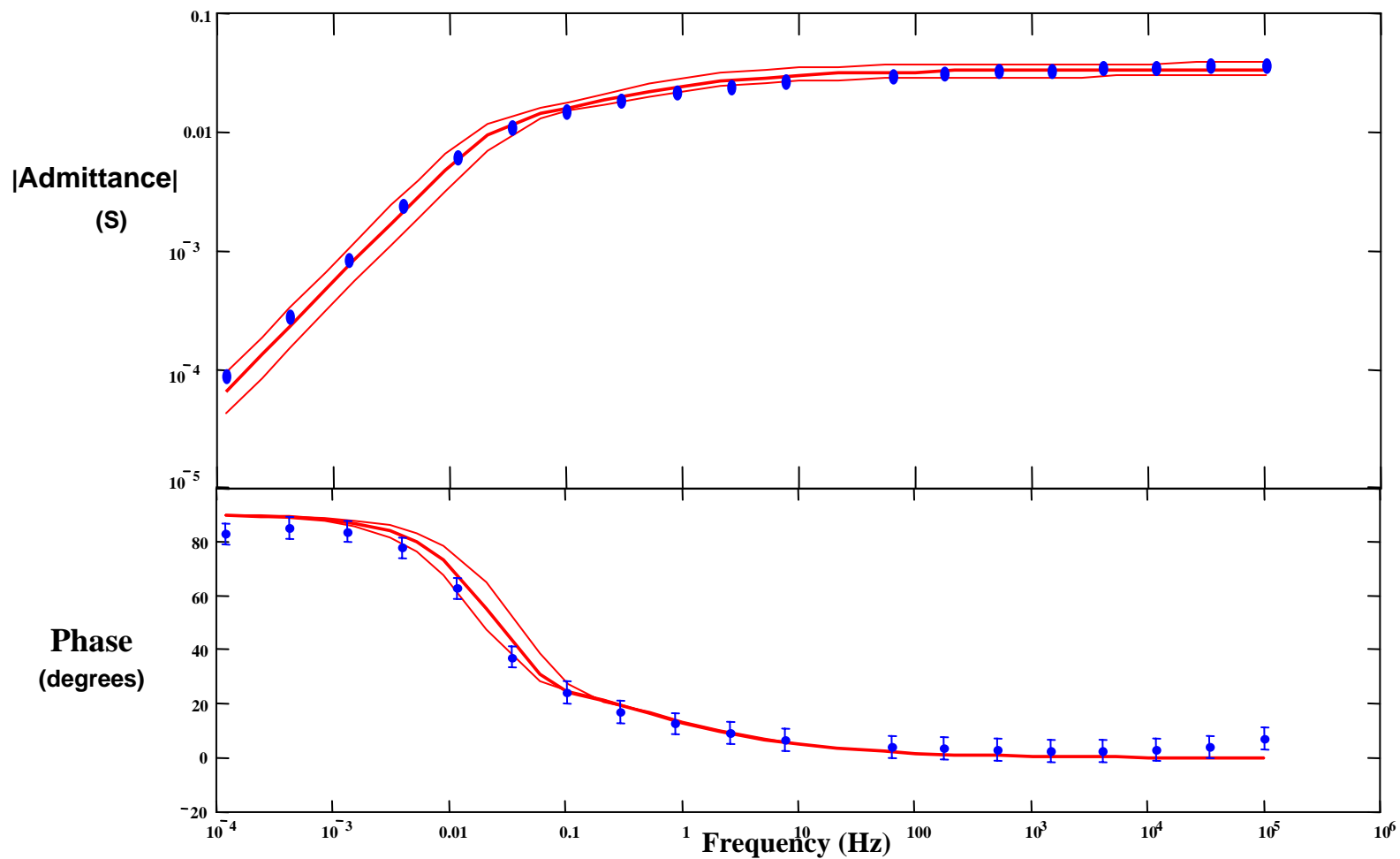


Figure 13: Admittance of an 8.5 μm thick polypyrrole film (blue dots), and a model fit (red lines). The thin red lines represent the bounds on the model imposed by independently measured variables. The diffusion coefficient is the one free parameter, and is estimated to be $2.1 \pm 0.7 \times 10^{-12} \text{ m}^2 \cdot \text{s}^{-1}$.

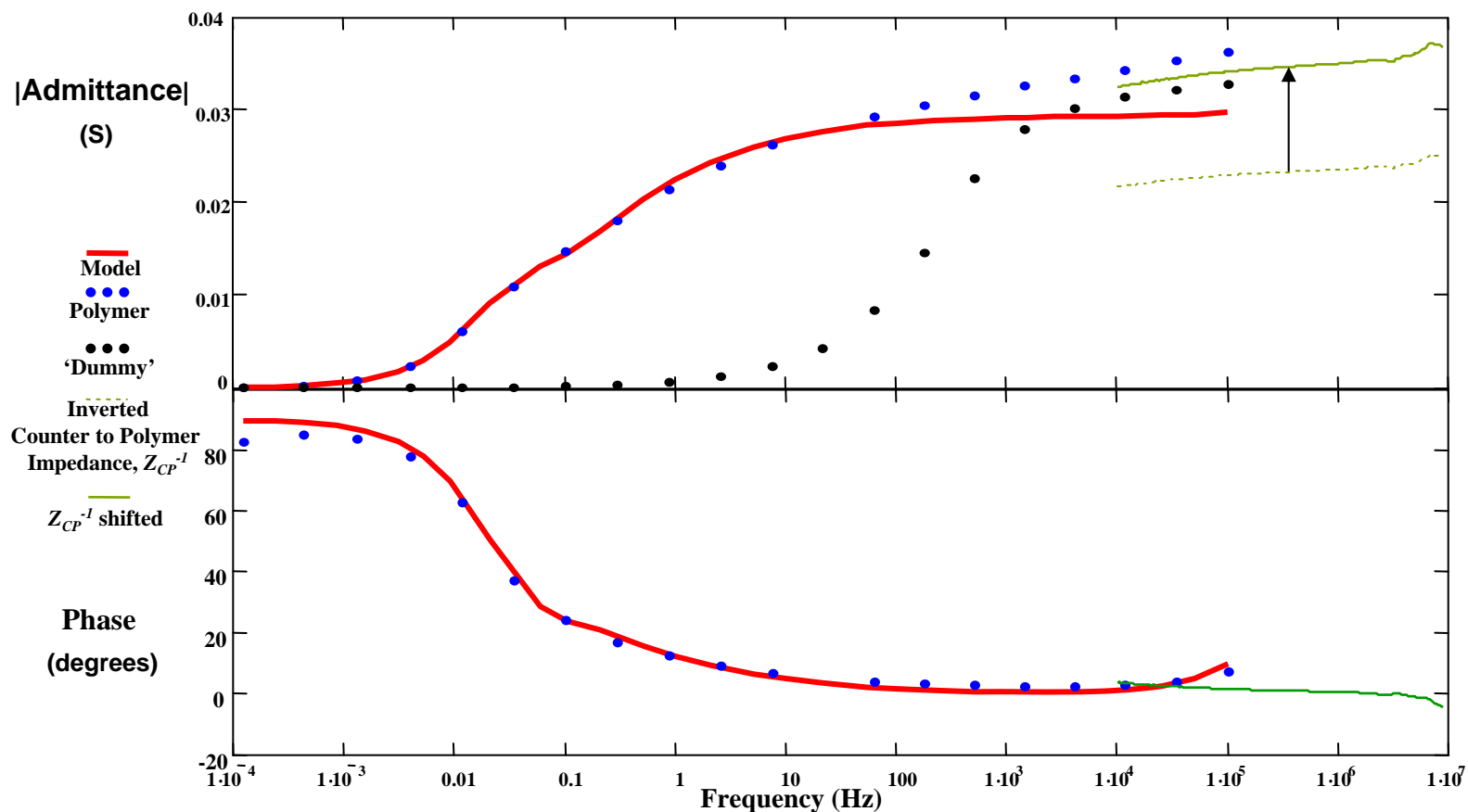


Figure 14: Repeat of Figure 13, but with the magnitude of admittance shown on a linear scale. Also shown is the measured impedance between the counter electrode and the polymer (green dash), and its value shifted down in resistance (solid green), for better comparison with the measured reference to polymer admittance. The black dots represent the admittance of a stainless steel electrode. The red line is a model fit, including the effects of finite gain and parasitic capacitances.

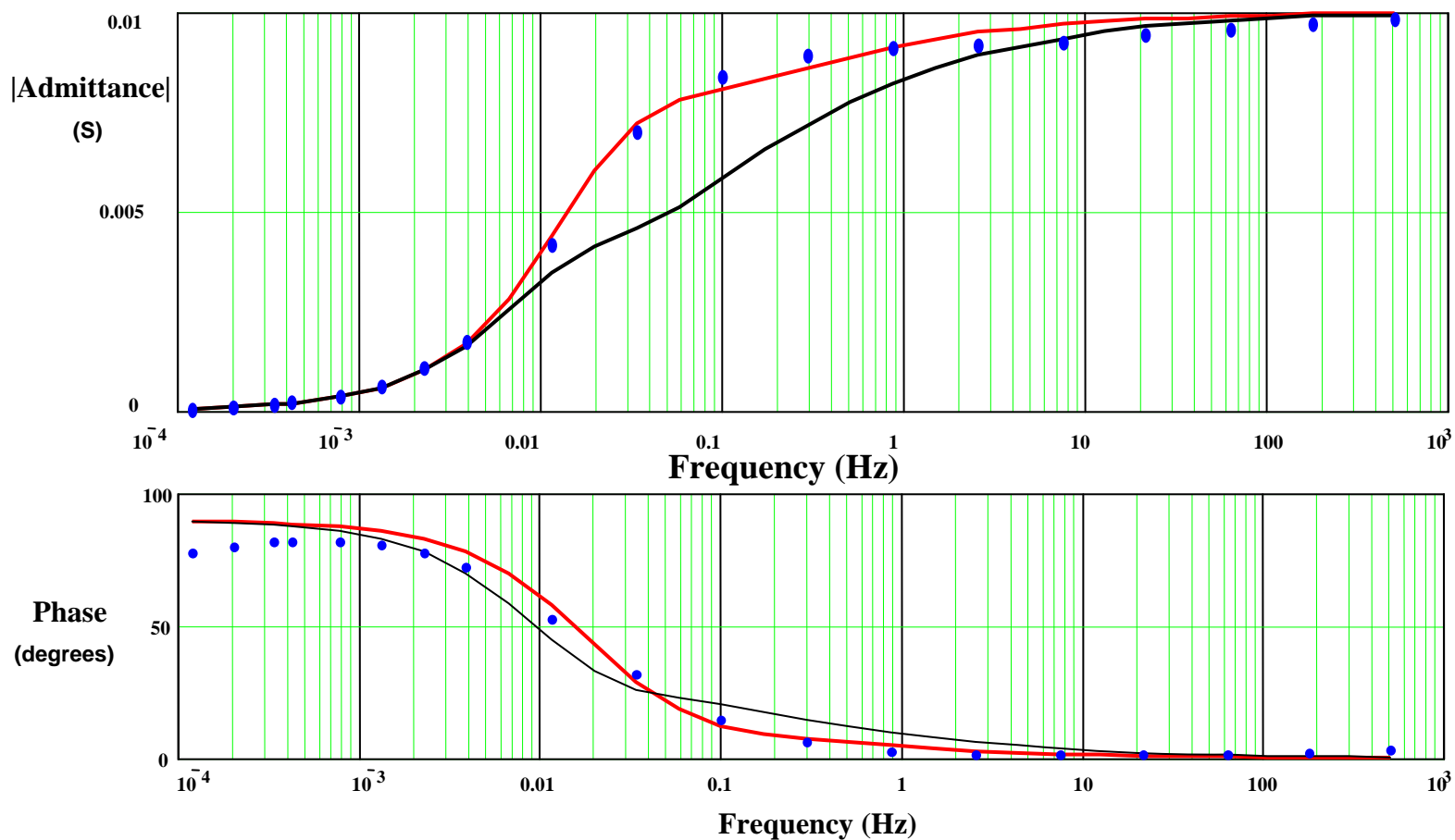


Figure 15: Admittance and electrolyte concentration. Admittance of an 8.5 μm thick polypyrrole film in 0.05 M tetraethylammonium hexafluorophosphate electrolyte (blue dots), and a model prediction using the same diffusion coefficient obtained from results in 0.3 M solution (red line), and a diffusion coefficient by the ratio of electrolyte conductivities (black line), as predicted for a “porous metal”.

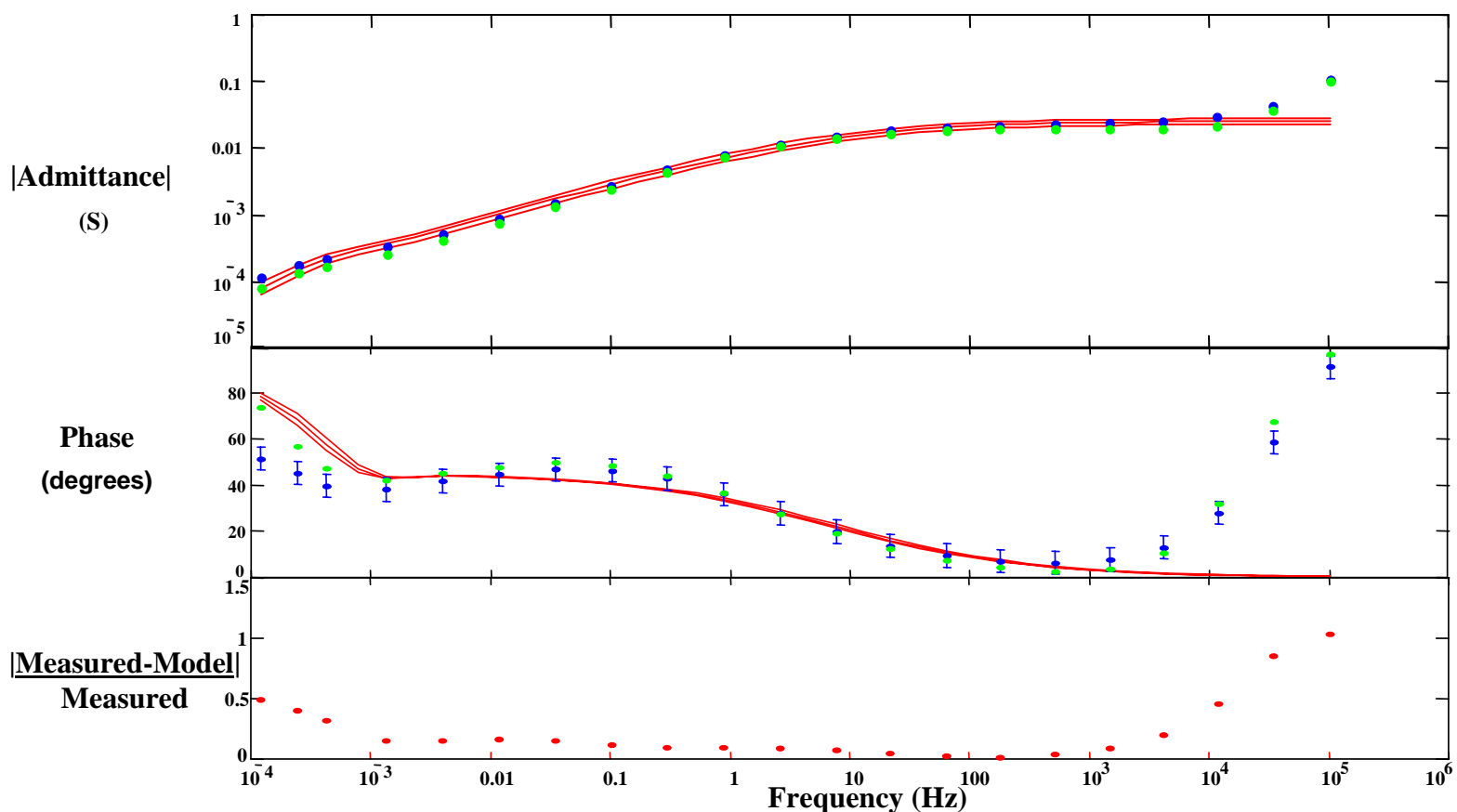


Figure 16: Admittance of a 44 μm thick polypyrrole film in 0.3 M tetraethylammonium hexafluorophosphate electrolyte (blue dots), and model fit with diffusion coefficient $D=0.6 \times 10^{-12} \text{ m}^2 \cdot \text{s}^{-1}$. The three red lines are used to indicate the mean and range of the fit curves due to uncertainties in the measured parameters. The bottom plot shows the magnitude of the difference between the mean model prediction and the measured values. $V_{eq} = -0.43 \text{ V}$ vs Ag/AgClO_4 .

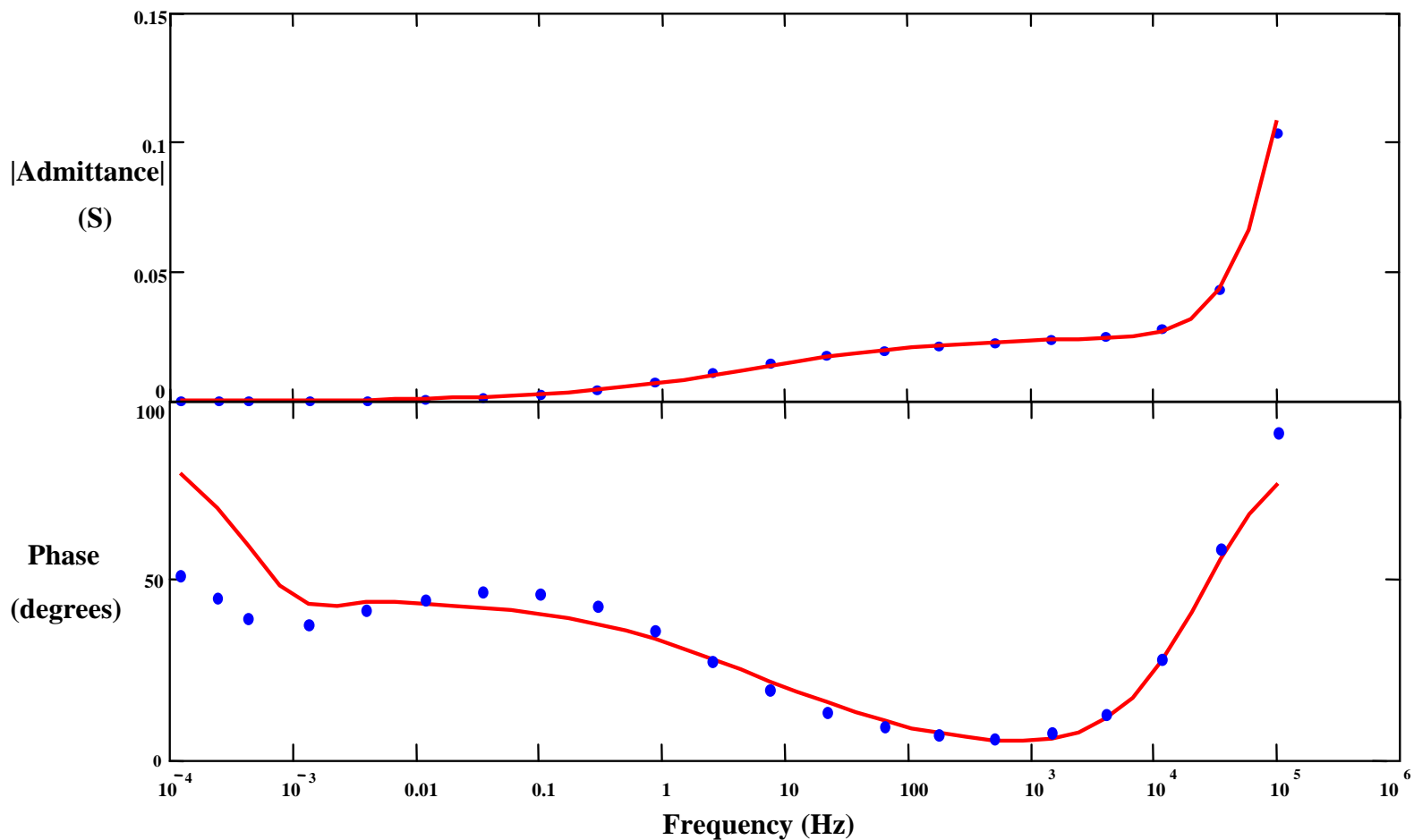


Figure 17: Admittance (blue dots) and a model fit (red lines), accounting for parasitic capacitance at high frequencies. The same data is shown as in Figure 16. The stray capacitance of 100 pF appears to be result of the finite input impedance of the Dynamic Signal Analyzer (HP3562A).

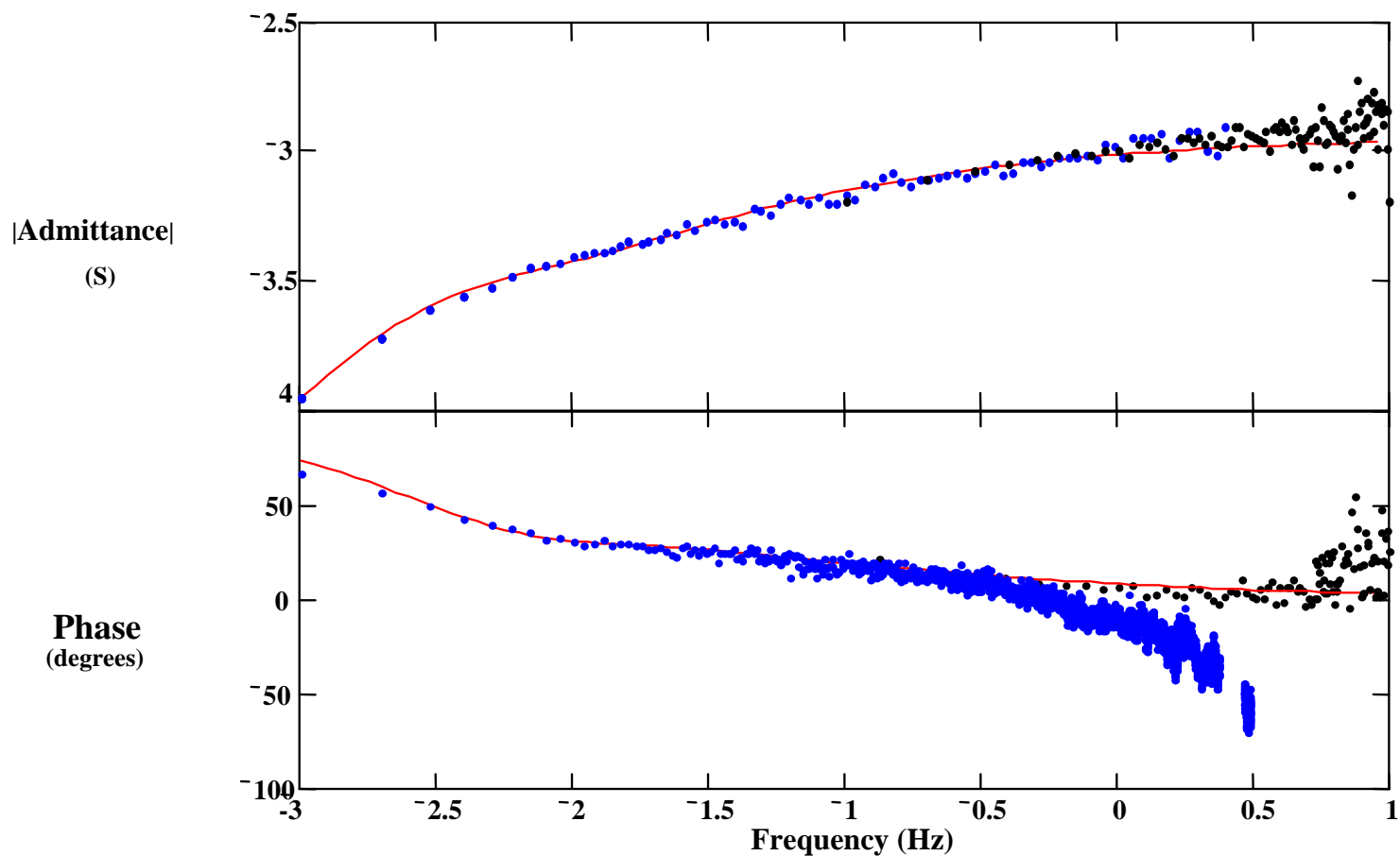


Figure 18: Admittance from a step response measurement on a 52 μm thick polypyrrole film in 0.05 M tetraethylammonium hexafluorophosphate electrolyte sampled at 10 Hz (blue dots) and 100 Hz (black dots). To obtain the model fit (line), both D , and R are adjusted. The diffusion coefficient, D is estimated to be $7 \pm 1 \times 10^{-12} \text{ m}^2 \cdot \text{s}^{-1}$. The applied step is 0.2 V about -0.19 V vs. Ag/AgClO_4 .

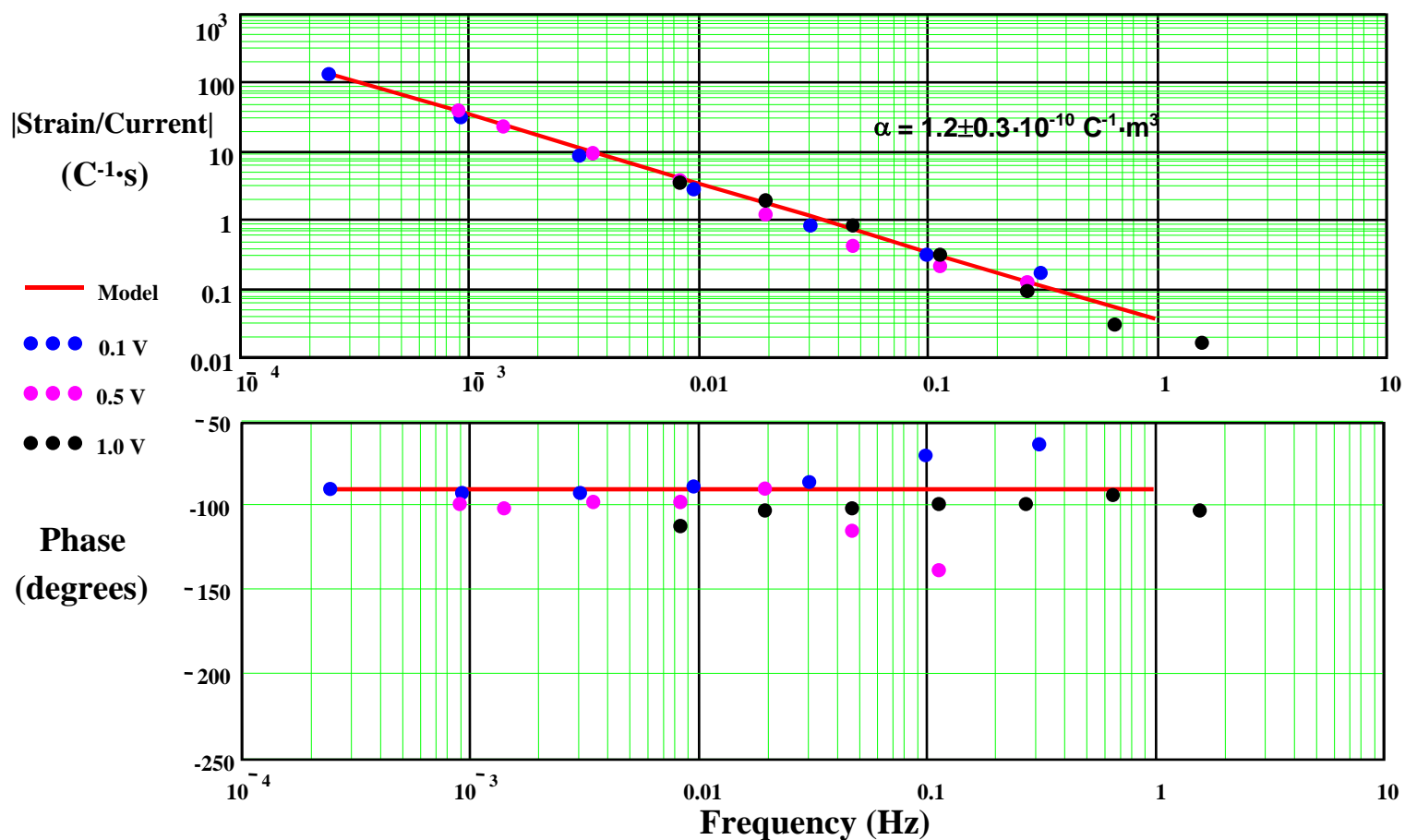


Figure 19: Strain to current transfer function showing the linearity of response. Data is from an 8.5 μm thick film in 0.37 M tetraethylammonium hexafluorophosphate, propylene carbonate with applied peak voltages of 0.1 V (blue), 0.5 V (magenta) and 1.0 V (black) about -0.2 V vs. Ag/AgClO_4 under isotonic conditions (1 MPa). Red lines represent a fit assuming a constant strain to charge ratio.

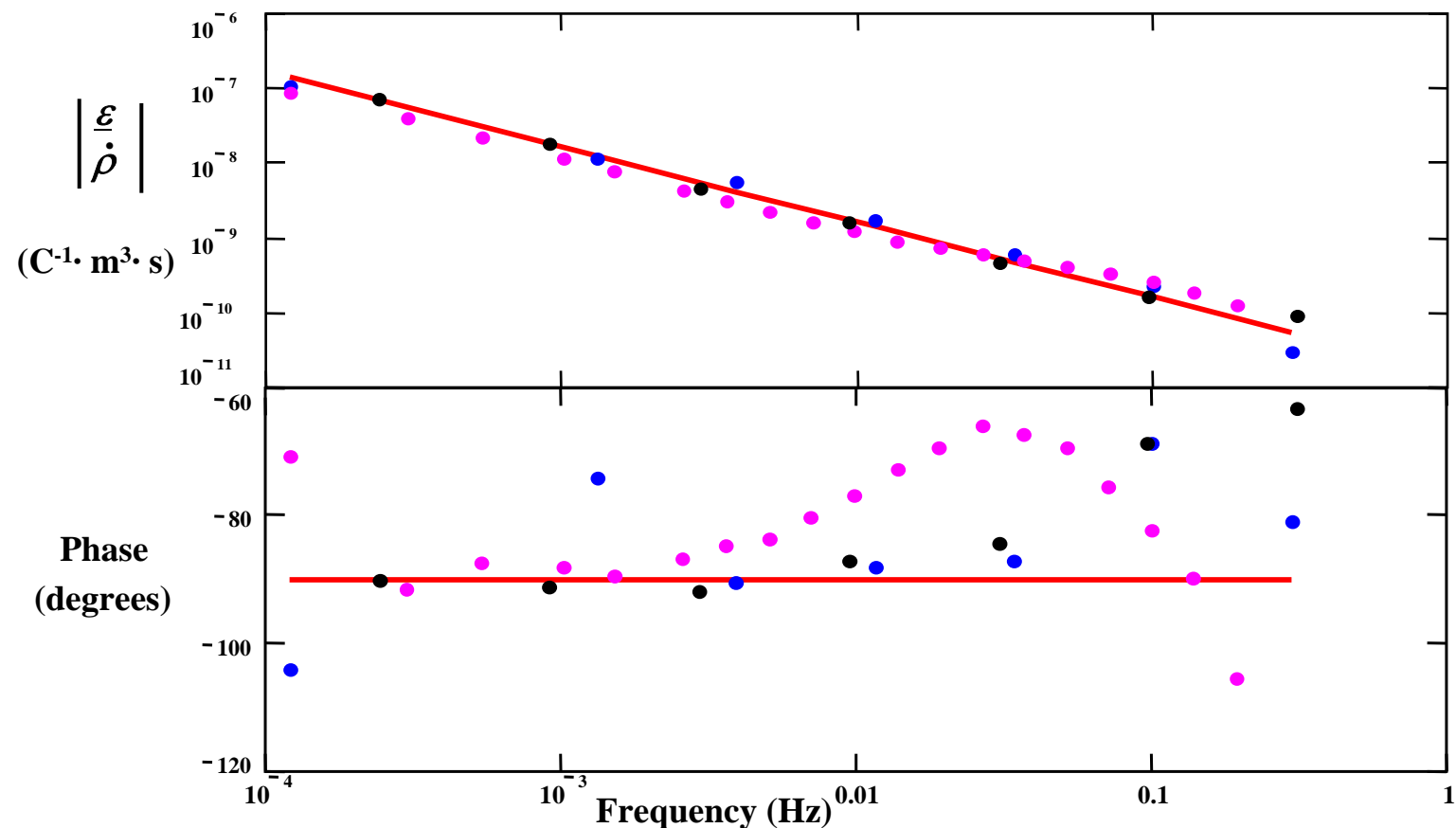


Figure 20: Strain, ε , to current density, ρ , transfer function from various films held at 1 to 4 MPa in tetraethylammonium hexafluorophosphate, propylene carbonate electrolyte, with 0.1 Vpk applied. Blue dots: 44 μm thick, 0.3 M, about -0.43 vs. Ag/AgClO_4 ; Magenta 12.5 μm , 0.3 M, -0.2 vs. Ag/AgClO_4 ; Black 8.5 μm , 0.37 M, -0.2 vs. Ag/AgClO_4 . The model represents a strain to charge ratio of $1.0 \times 10^{-10} \text{ m}^3 \cdot \text{C}^{-1}$, and all points lie in the range of 0.7 - $1.4 \times 10^{-10} \text{ m}^3 \cdot \text{C}^{-1}$.

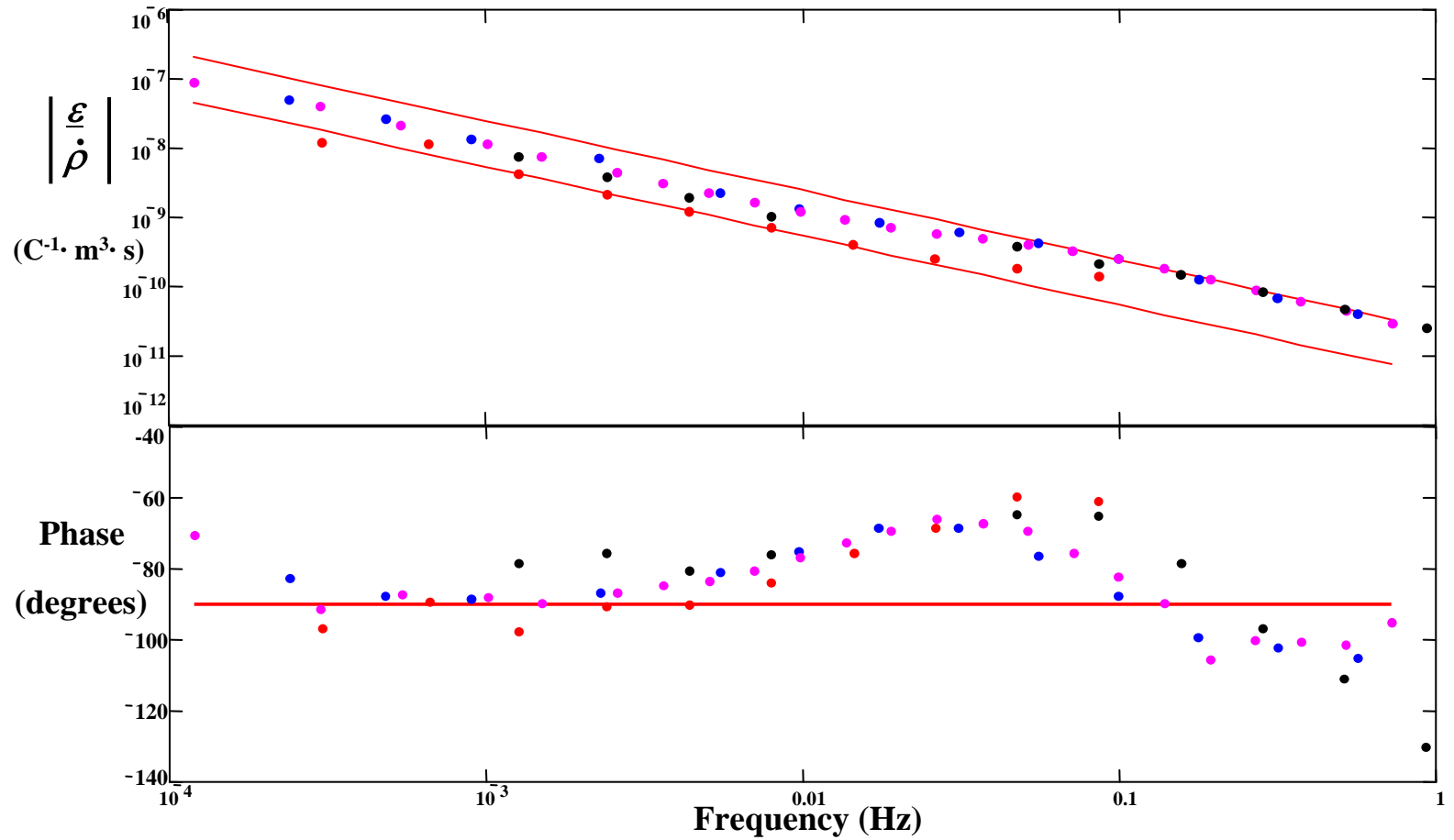


Figure 21: The effect of stress and time on the strain produced per unit charge. Strain to current transfer functions for three isotonic conditions, 4 MPa (blue and magenta), 30 MPa (black) and 40 MPa (red dots). The upper red line in the magnitude plot corresponds to a strain to charge ratio of $1.5 \times 10^{-10} m^3 \cdot C^{-1}$, and the lower line $0.4 \times 10^{-10} m^3 \cdot C^{-1}$.

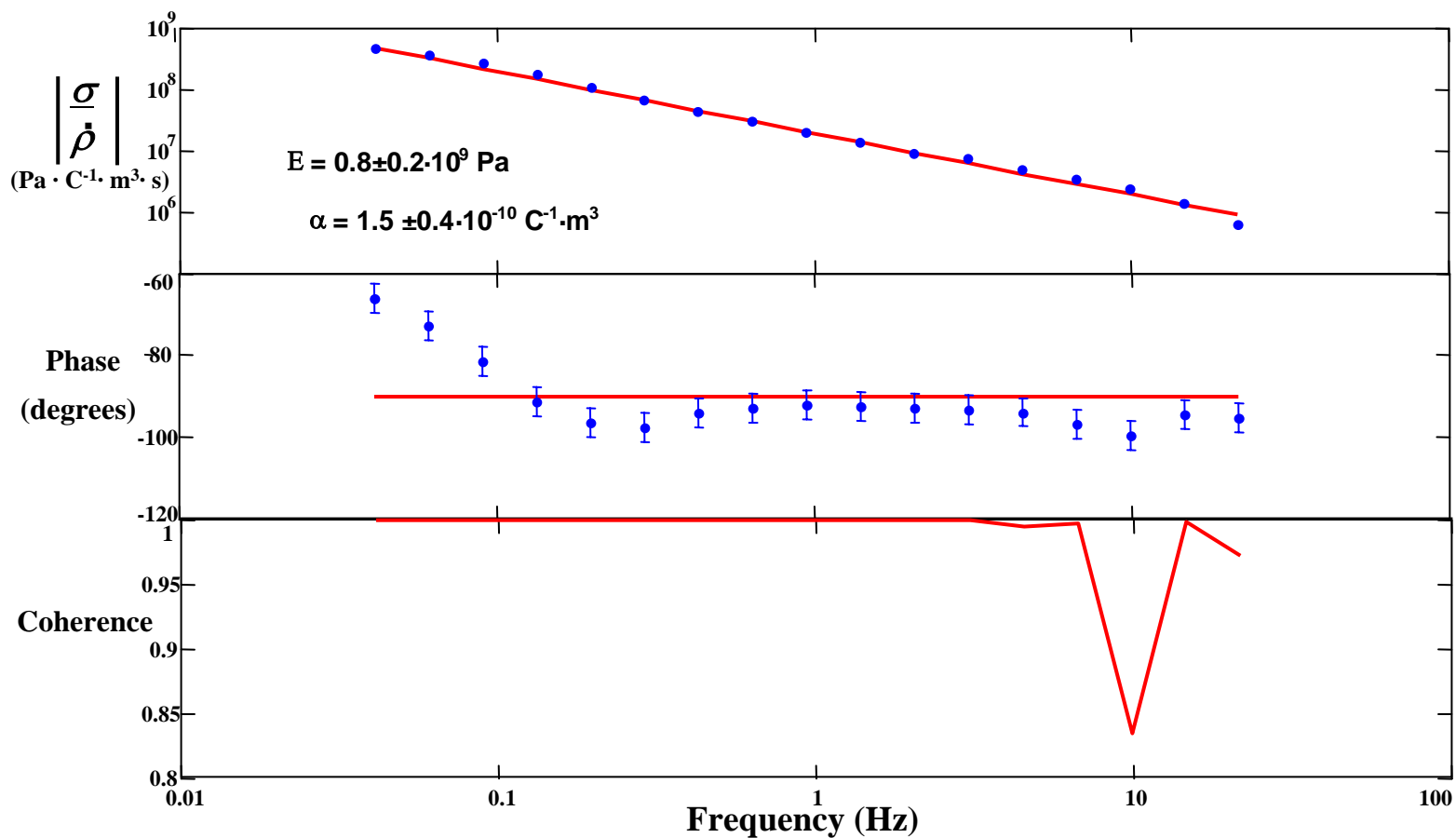


Figure 22: Stress to current transfer function for an 12.5 μm thick film in 0.3 M tetraethylammonium hexafluorophosphate, propylene carbonate. A 0.1 V peak voltage amplitude was applied about -0.2 V vs. Ag/AgClO_4 . Division of the slope by the elastic modulus predicts a strain to charge ratio of $1.5 \pm 0.4 \text{ m}^3 \cdot \text{C}^{-1}$. The data shown is the result of 100 averages, with the coherence shown in the bottom plot.

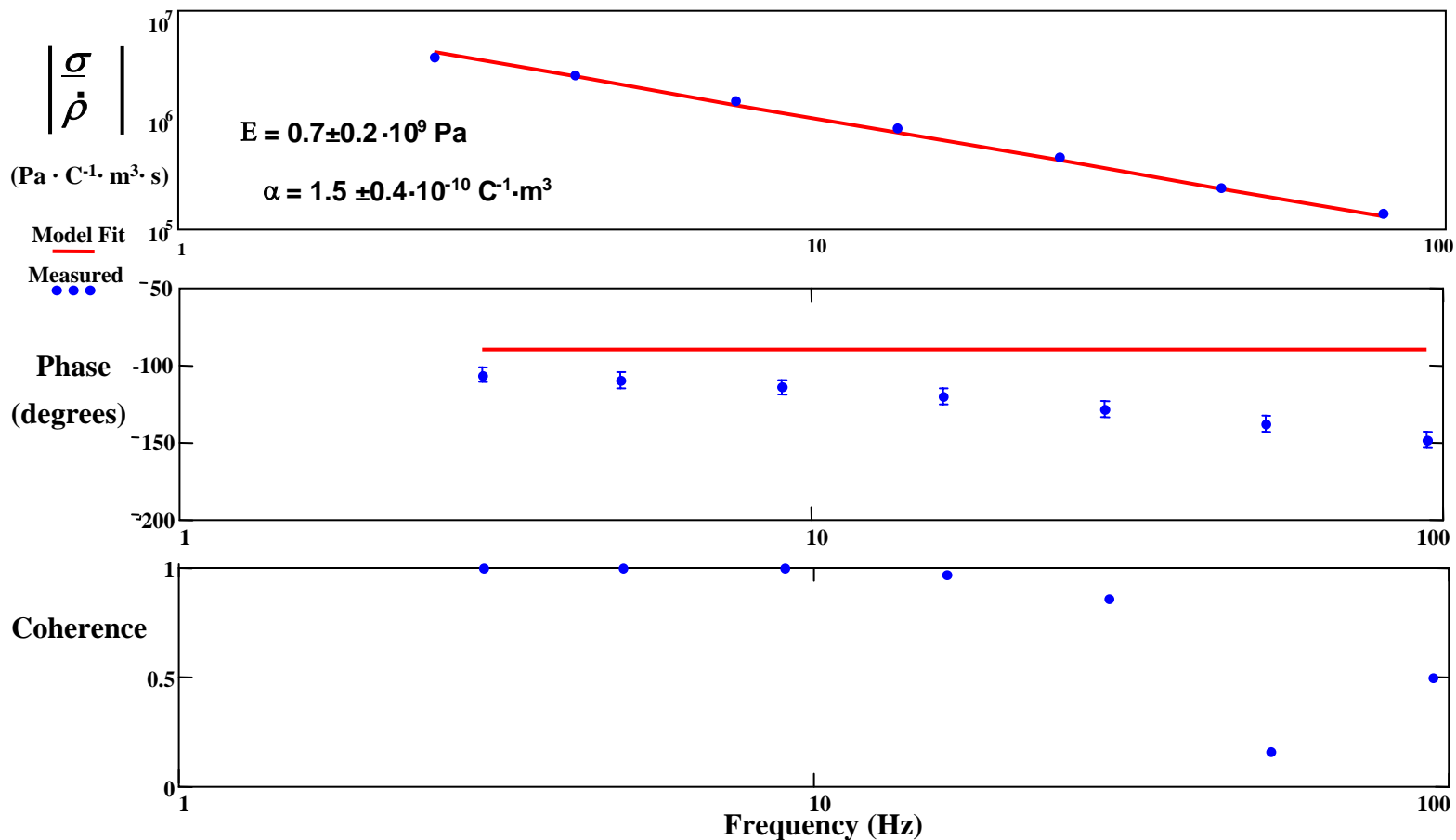


Figure 23: Stress to current transfer function for an 8.5 μm thick film in 0.37 M tetraethylammonium hexafluorophosphate, propylene carbonate. A 1.4 V peak amplitude was applied about -0.2 V vs. Ag/AgClO_4 . Division of the slope by the elastic modulus predicts a strain to charge ratio of $1.5 \pm 0.4 \text{ m}^3 \cdot \text{C}^{-1}$. The data shown is the result of 1000 averages, with the coherence shown at the bottom.

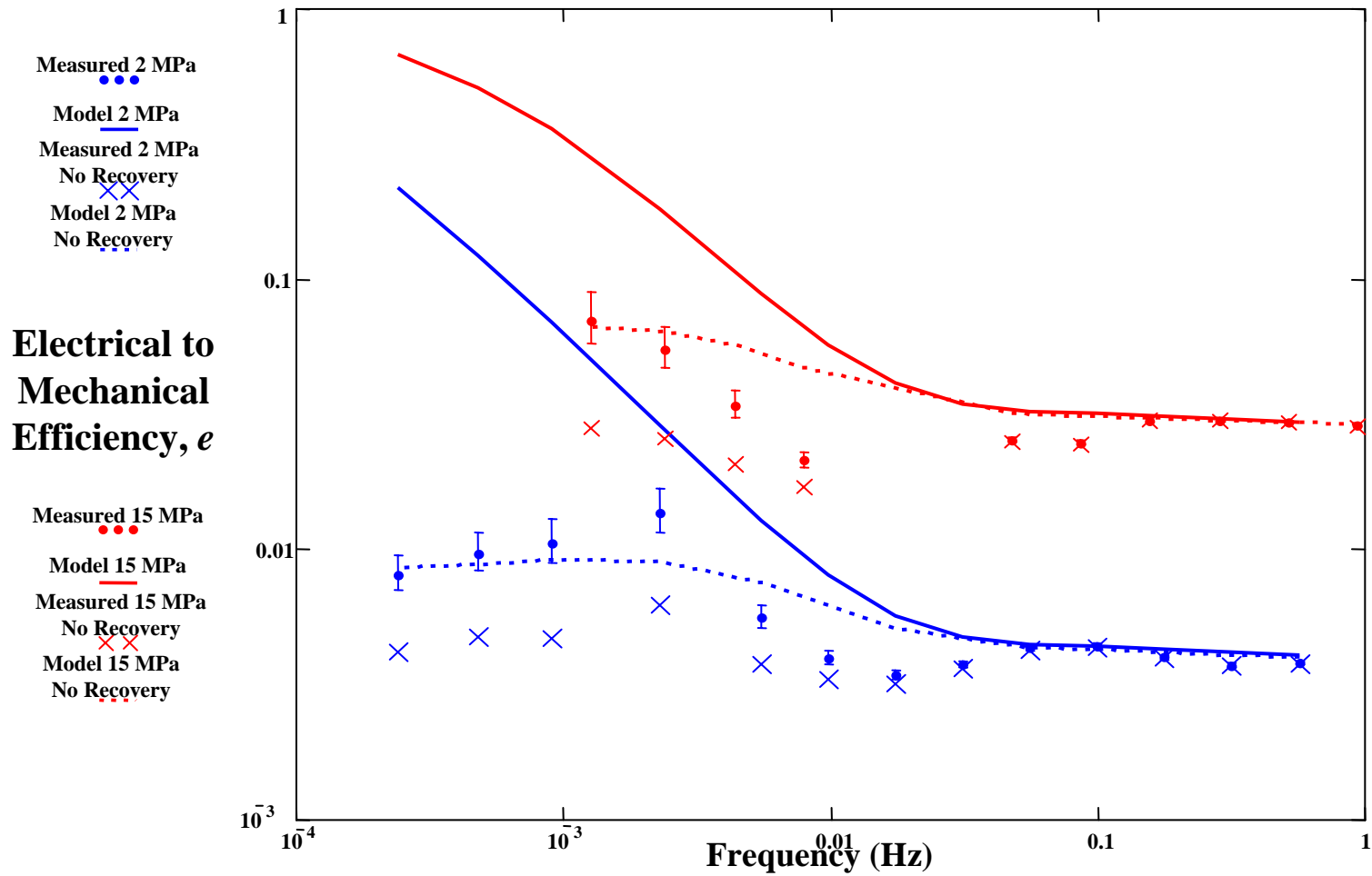


Figure 24: Electrical to mechanical actuator efficiency. Modeled (lines) and measured efficiencies under isotonic stresses of 4 MPa (blue) and 30 MPa (red). The dashed line models and X data assume no energy recovery, while the point data and solid line models assume that stored energy is recovered.